

## **THE PERFORMANCE AND OPTIMISATION OF A NOVEL FAÇADE PANEL FOR ENERGY-EFFICIENT BUILDINGS**

Q. JIN<sup>1</sup>; M. OVEREND<sup>1</sup>; M. KRAGH<sup>2</sup>

*1: Department of Engineering, University of Cambridge, Trumpington Street, Cambridge, CB2 1PZ, UK*

*2: Arup, 13 Fitzroy Street, London, W1T 4BQ, UK*

### **ABSTRACT**

A suitable multi-criterion optimisation method is identified and deployed to optimise a cellular spandrel panel for a high performance fibre reinforced polymer (FRP) façade, with the objective to minimise the construction and in-service energy costs. Furthermore, the significance of various façade components to the overall thermal performance is identified and compared.

### **INTRODUCTION**

The in-service performance of commercially available curtain walling systems has undergone steady progress over the recent decade chiefly through the technological developments of high performance glazing. The improvements are such that the principal factor that limits the thermal performance is currently the framing, which is typically based on the use of thermally broken aluminium extrusions. However, the industry-standard combination of aluminium frames and the glazing edge conditions leads to thermal losses and relatively high thermal transmittance (U-value).

Fibre reinforced polymer (FRP) is a relatively novel construction material with several advantageous properties, such as high specific strength and stiffness, low thermal conductivity, high corrosion and weather resistance. Its use in facades, therefore, provides the opportunity to reduce the number of parts (compared with aluminium-based systems) due to the absence of thermal breaks, which may in turn bring a step-change to curtain wall thermal performance and energy efficiency of buildings.

A façade prototype was proposed by Arup (Figure 1<sup>[1]</sup> and Figure 2), the U-value of which easily achieves the target of  $1.3\text{W/m}^2\text{K}$ . It consists of four main component types, i.e. glazing, spandrel panel, mullions, and joints (where joints include the pultruded FRP profiles which are used at the interfaces between the components). All the components, with the exception of the glazing, are pultruded FRP profiles. Arup have done some structural calculations<sup>[1]</sup>, in which the cellular panel was modelled as a continuous beam on short columns. Thermal performance was also investigated by Arup using BISCO software. The effects of the number of webs were assessed<sup>[2]</sup>, with the assumption that the cavities were filled completely with aerogel, while the possibility and feasibility of partly filling the gap was not considered.

This study aims to develop a method to optimise the spandrel panel on the façade module proposed by Arup in terms of the structural and thermal performance, with the objective of minimising the total cost of construction and energy consumption. In doing so, it is necessary to construct accurate analytical and numerical models that predict the structural and thermal performance. Finite element analysis is performed to investigate and optimise the structural

performance using ANSYS v11.0 and an analytical model for thermal analysis is constructed in MATLAB v7.6.0. Finally, an office building is modelled by Virtual Environment v5.9 to evaluate and compare the total costs and eventually to outline a method for determination of the optimal solution.

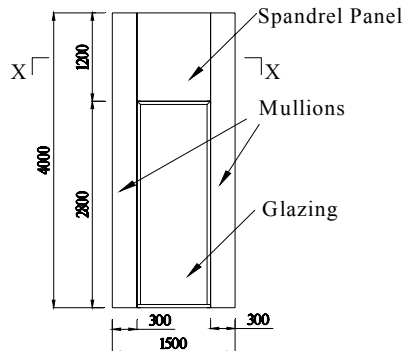


Figure 1: Front elevation of an FRP façade module, which consists of glazing, spandrel panel, mullions and joints.

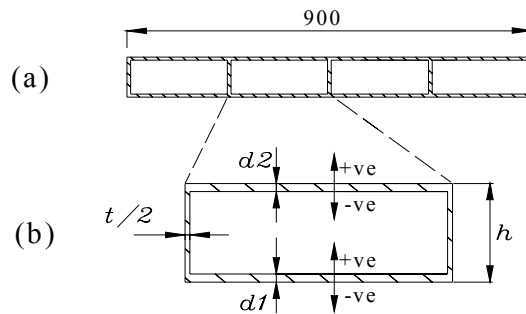


Figure 2: Cross-section of a cellular spandrel panel: (a) plan view X-X; (b) a single cell;  $d1$  denotes the thickness of the external skin and  $d2$  denotes that of the internal skin. The arrows denote sign convention.

## STRUCTURAL ANALYSIS AND RESULTS

Two, three, four-cell spandrel panels, each measuring 900mm (W)  $\times$  1200mm (H), are investigated. Material properties are taken from manufacturers' data [3], which are valid for a temperature range of -20°C to 60°C.

Four load cases (Table 2) are considered to satisfy CWCT standards [4], and load case combinations are shown in Table 3.

|         | Description   |
|---------|---|
| WL      | Uniformly distributed wind load of $\pm 2.4 \text{ kN/m}^2$ , acting externally   |
| DL      | Uniformly distributed load of $1.0 \text{ kN/m}^2$ , acting internally  |
| HLL     | A horizontal line load of $0.74 \text{ kN/m}$ acting at a height of 1.1m above the finished internal floor level, acting internally |
| PLI/PLE | A point load of $0.5 \text{ kN}$ applied with a contact area of $100 \text{ mm}^2$ square, acting internally/externally             |

Table 2: Load cases.

| Serviceability Limit State |             | Ultimate Limit State |   |
|----------------------------|-------------|----------------------|---|
| I                          | (WL)+(DL)   | i                    | $1.5 \times (\text{WL}) + 1.5 \times (\text{DL})$   |
| II                         | (WL)+(HLL)  | ii                   | $1.5 \times (\text{WL}) + 1.5 \times (\text{HLL})$  |
| III                        | (-WL)+(PLI) | iii                  | $1.5 \times (-\text{WL}) + 1.5 \times (\text{PLI})$ |
| IV                         | (WL)+(PLE)  | iv                   | $1.5 \times (\text{WL}) + 1.5 \times (\text{PLE})$  |

Table 3: Load case combinations.

Three constraints are identified:

- The thicknesses  $d1$ ,  $t$ ,  $d2$  are no less than 4mm, and should be increased at an interval of 0.5mm due to manufacture limitations;  $h$  ranges from 23mm to 120mm;
- Stresses at any point should not exceed the allowable stresses;
- The out-of-plane allowable deflection should be no more than 6mm (span/200).

Finite element analysis and optimisation are performed by ANSYS v11.0. Firstly, an initial model is built. And then zero-order optimisation method is applied with the assumption that

the control variables are continuous. Finally, the optimal solution is adjusted according to manufacturing requirements, using direct search method from Hooke and Jeeves<sup>[5]</sup>. Optimal solutions are presented in Table 4.

|                                       |                        |         | Constraints          | 2 cells | 3 cells | 4 cells |
|---------------------------------------|------------------------|---------|----------------------|---------|---------|---------|
| Critical load cases combination       |                        |         | -                    | III     | IV      | IV      |
| Normal Stresses (MPa)                 | Along-fibre direction  | Maximum | 185                  | 29      | 30      | 26      |
|                                       |                        | Minimum | -185                 | -32     | -37     | -40     |
|                                       | Across-fibre direction | Maximum | 77                   | 20      | 27      | 26      |
|                                       |                        | Minimum | -77                  | -22     | -28     | -27     |
| Maximum Shear Stress(MPa)             |                        |         | 19                   | 6       | 8       | 5       |
| Deflection(mm)                        |                        |         | 6                    | 6       | 6       | 6       |
| $d1$ (mm)                             |                        |         | $d1 \geq 4$          | 6.5     | 4.5     | 4       |
| $d2$ (mm)                             |                        |         | $d2 \geq 4$          | 6       | 4       | 4       |
| $t$ (mm)                              |                        |         | $t \geq 4$           | 5.5     | 4.5     | 4       |
| $h$ (mm)                              |                        |         | $23 \leq h \leq 120$ | 68      | 52.5    | 35      |
| Cross-section Area (mm <sup>2</sup> ) |                        |         | -                    | 12019   | 8661    | 7636    |

Table 4: Optimal structural solutions for spandrel panel

## Discussion

Load cases combination III/IV are critical, because the point load (PL), which stems from maintenance, e.g. a cleaning cradle resting against the wall or a person standing on a ladder leaning against the facade, results in a much larger deflection than other load cases. Small increases in  $d1$  significantly reduce the deflection induced by the point load (PL).

Deflection constraint is always active, leaving large differences between the actual stresses and the allowable stresses. Therefore, future work could involve balancing the stiffness and strength by changing the material and the aspect ratio of the fibres, the material of the matrix, the fibre-matrix volume ratio or manufacturing methods, which might potentially lead to a further reduction of material cost.

A two-cell panel requires the largest volume of FRP, because the number of webs reduces to such a level that both  $d1$  and  $d2$  need to be increased substantially to keep the deflection within the limits. However, this could be an advantage because the number of thermal bridges is reduced.

## THERMAL ANALYSIS AND RESULTS

### Spandrel Panel

The initial thermal performance objective is a total U-value of 1.3W/m<sup>2</sup>K, which means if other components are kept as originally designed, the U-value of the spandrel panel should be 1.7W/m<sup>2</sup>K. One cell is simplified as a vertical cavity within an FRP enclosure. Indoor and outdoor temperatures are assumed to be 20°C and 0°C respectively. Conduction, natural convection, radiation are all considered to form the network. The convection heat transfer between the webs and the air is considered negligible for two reasons: firstly, since the conductivity of aerogel is extremely low, the temperature difference across the enclosed air cavity is very small- within 6K. Secondly, based on previous work<sup>[6]</sup>, the aspect ratio of the cavity is sufficient to make the effects of the vertical webs negligible.

An analytical model, which can be used to predict the U-value under different geometric parameter combinations, is constructed in MATLAB v7.6.0. However, the U-value cannot be

brought down below  $2.5 \text{ W/m}^2\text{K}$  by only adjusting the parameters in the feasible design region. Therefore, an insulation layer of aerogel is inserted to improve the thermal performance. The simplified network is presented in Figure 3.

Surface conductances are determined according to EN ISO 6946 [7]. Effective conductance for the natural convection of the air is calculated according to Yin et al [6]. Effective conductances for thermal radiation between the outside FRP skin, the webs, and the surface of the insulation layer are calculated according to Holman [8].

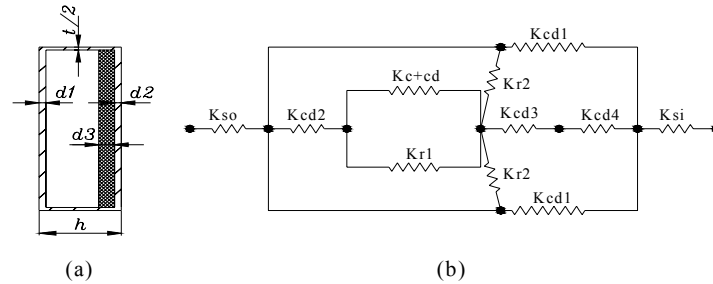


Figure 3: (a) Cross-section of one cell,  $d3$  denotes the thickness of aerogel insulation layer; (b) Simplified network. ( $K_{cd}$ ) conductance of FRP or aerogel; ( $K_{c+cd}$ ) effective conductance for conduction and convection of the air in the cavity; ( $K_r$ ) effective conductance for radiation among the four enclosed FRP surfaces; ( $K_s$ ) surface conductance.

The analytical model shows that the U-value of the spandrel panel depends largely on the thickness of the aerogel layer, as shown in Figure 4, while the numbers of cells, the thickness of the FRP outside and inside skins, webs, and the depth of the air cavity all have little effects. For a three-cell panel, when 7.5mm aerogel is inserted, a U-value of approximately  $1.7 \text{ W/m}^2\text{K}$  can be achieved with  $h$  ranging from 35mm to 120mm (Case 1). However, the original design by Arup achieves an overall U-value of  $1.1 \text{ W/m}^2\text{K}$ , which requires the U-value of the spandrel panel to be  $0.4 \text{ W/m}^2\text{K}$ . This would require 100mm aerogel infill (Case 2). Figure 5 shows U-value of the structural optimal two-cell spandrel varies with the thickness of the insulation layer.

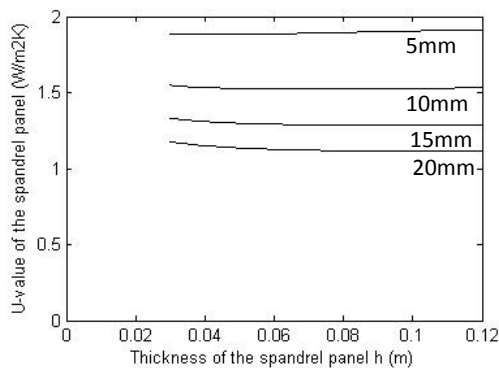


Figure 4: U-value of a three-cell spandrel panel with respect to several specific thickness of aerogel layer shown in mm and varying thickness.  $d1 = d2 = t = 4 \text{ mm}$ .

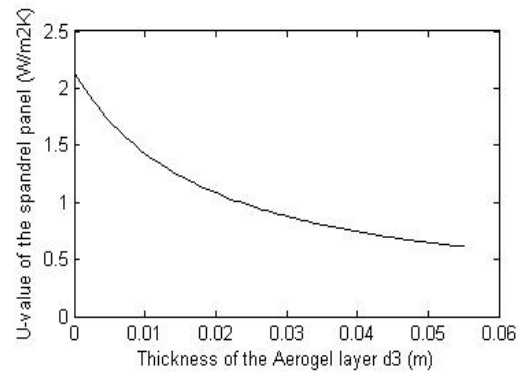


Figure 5: U-value of the optimal two-cell spandrel panel with increasing thickness of aerogel insulation layer.

## Building Energy Simulation

A simplified building energy simulation and cost comparison is undertaken to investigate a method for determination of the most cost effective design. A  $27 \text{ m} \times 27 \text{ m}$  five-floor office building is modelled using Virtual Environment v5.9. The building is assumed to be located

in London, and the façade service life is 25 years. The indoor temperature is maintained at 20°C throughout the year. The cost of FRP is trivial, so it is excluded at this stage. Discounted cash flow analysis is applied to calculate the annualised capital cost. The real discount rate is assumed to be 8% during a capital repayment period of 25 years, and the energy prices are assumed to be constant. Results are presented in Table 5.

|  |                 | Case 1 | Case 2 |
|--|-----------------|--------|--------|
| Total U-value (W/m <sup>2</sup> K)                   |                 | 1.3    | 1.1    |
| U-value for spandrel panel (W/m <sup>2</sup> K)      |                 | 1.7    | 0.4    |
| Energy cost per year                                 | Electricity (£) | 9.0k   | 8.7k   |
|  | Gas (£)         | 2.1k   | 2.6k   |
|  | Total (£)       | 11.1k  | 11.3k  |
| Energy cost per year per spandrel panel (£)          |                 | 31.3   | 31.0   |
| Cost for aerogel per spandrel panel (£)              |                 | 15.5   | 208.8  |
| Cost for aerogel per spandrel panel for Year One (£) |                 | 1.5    | 19.6   |
| Total annualised cost for Year One (£)               |                 | 32.8   | 50.6   |

Table 5: Cost comparison when the U-value of the façade is 1.3W/m<sup>2</sup>K and 1.1 W/m<sup>2</sup>K.

By comparing the two cases, it is clear that a more economic way is to use a thin layer of aerogel rather than completely filling the cavity. Therefore, basing on the structural optimal solutions, insert a minimal thickness of aerogel which can achieve the U-value of 1.7W/m<sup>2</sup>K for the spandrel panel. Results are shown in Table 6.

|  |             | 2 cells | 3 cells | 4 cells |
|--|-------------|---------|---------|---------|
| FRP cross-section area (mm <sup>2</sup> )      |             | 12019   | 8661    | 7636    |
| Minimal thickness of aerogel $d_3$ (mm)        |             | 6.5     | 7.5     | 8       |
| U value of spandrel panel (W/m <sup>2</sup> K) |             | 1.7     | 1.7     | 1.7     |
| Cost per spandrel panel for Year One           | FRP (£)     | 0.01    | 0.01    | 0.01    |
|  | Aerogel (£) | 1.3     | 1.5     | 1.6     |
|  | Energy (£)  | 31.3    | 31.3    | 31.3    |
| Total annualised cost for Year One (£)         |             | 32.6    | 32.8    | 32.9    |

Table 6: Cost comparison for the structural optimal spandrel panels.

## Discussion

Figure 6 shows how the total U-value changes with each component when others are kept unchanged as originally designed. With the lowest gradient, the spandrel panel is the least effective component for changing the overall U-value of the façade module. Figure 7 shows that the joints are the main heat-losing components. Therefore, it would be far more beneficial to improve the thermal performance of the joints.

The price of aerogel is around £2/litre. Since the U-value of the spandrel panel does not affect that of the whole façade as much, it is not economic to fill the cavity completely with aerogel to improve the total U-value slightly. However, it is worth inserting a thin layer of aerogel. In addition, aerogel is being considered only due to an aspiration to develop a translucent façade system, but when translucency is not required or feasible, other more economic insulation materials may be used instead. Future work will seek to identify the viable costs of insulation.

The energy cost model is a highly simplified one which is used to identify the most economic solution by comparing the differences among the candidates. The study explores the methodology rather than aiming to obtain the accurate energy cost. Future work will involve constructing a more comprehensive and practical model to predict the actual energy cost.

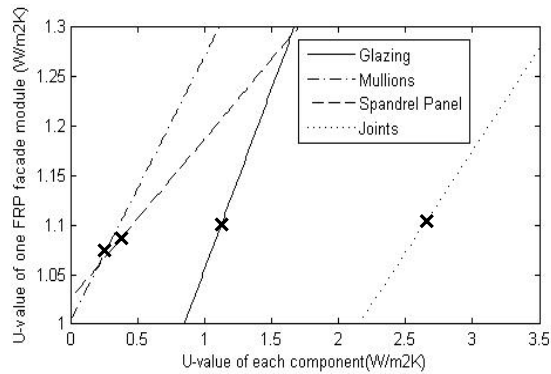


Figure 6: U-value relationships between each component and one FRP façade module, when other components are kept unchanged. The original design value is denoted by x.

Thermal Conductance of each component (W/K)

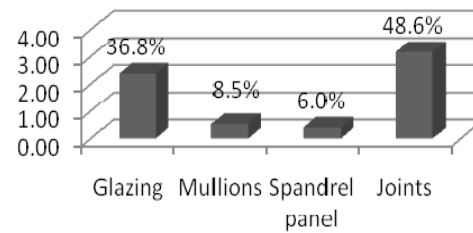


Figure 7: Energy loss through each component for one façade module (original design).

## SUMMARY

3-D spandrel panels are modelled and the optimal geometric parameter combinations are obtained. Knowing that the point load (PL) is critical and the deflection constraint is always active, structural optimisation is achieved in the first instance to determine the cross-section of the spandrel panel. The air cavity is subsequently filled with a thin layer of aerogel to satisfy the thermal insulation and translucency requirements. Future work should focus on improving the thermal performance of the joints.

## ACKNOWLEDGEMENTS

The first and second authors wish to express their gratitude to the third author and his team at Arup for their helpful guidance and suggestions throughout the whole project. The initial FRP façade concept was developed as part of the collaborative project The Integrated Building Envelope ([www.integratedbuildingenvelope.com](http://www.integratedbuildingenvelope.com)) with support from Building Lab DK and Realdania.

## REFERENCES

1. Arup: Internal technical report: Structural calculation (draft 4), London, UK, 2008.
2. Arup: Internal technical report: Fibre reinforced spandrel- thermal performance assessment, London, UK, 2007.
3. Fiberline Composites A/S: Fiberline design manual, Denmark, 2003.
4. Centre for Window & Cladding Technology: Standard for curtain walling 2<sup>nd</sup> edition, Bath, UK, 1996.
5. Hooke, R. and Jeeves, T.A.: Direct search solution of numerical and statistical problems, Westinghouse Research Laboratories, Pittsburgh, Pennsylvania, USA, 1960.
6. YIN, S. H. et al: Natural convection in an air layer enclosed within rectangular cavities. Int. J. Heat Mass Transfer, Vol 21, pp.307-315, UK, 1978.
7. The International Organization for Standardization: EN ISO 6946, Building components and building elements- Thermal resistance and thermal transmittance- Calculation Method, Brussels, 2007.
8. Holman, J.P.: Heat transfer 9<sup>th</sup> edition, pp376-384, New York, USA, 2002.